

Analysis of Coupling Phenomena between Spacecraft Antennas based on Equivalent Current Technique

L. Salghetti Drioli
European Space Agency (ESA/ESTEC),
2200AG Noordwijk, The Netherlands
Luca.Salghetti.Drioli@esa.int

L. J. Foged, F. Saccardi, L. Scialacqua
Microwave Vision Italy (MVI),
Via dei Castelli Romani 59, 00040, Pomezia, Italy
lars.foged@microwavevision.com
francesco.saccardi@microwavevision.com
lucia.scialacqua@microwavevision.com

Abstract— In this paper an advanced analysis regarding the interaction between antennas installed on a spacecraft is presented. In particular, data coming from a GNSS satellite near field measurement campaign have been considered and the MV-INSIGHT software has been used to perform the analysis. Such a software, starting from the measured field of a DUT, computes equivalent currents on a surface conformal to the test object. The availability of the equivalent currents is a key point for an in depth analysis of DUT such as a spacecrafts since it allows to obtain exclusive diagnostic information like coupling between antennas and satellite structure.

The near-field data have been collected in the Hybrid ESA RF and antenna Test Zone (HERTZ) at ESTEC. Such a hybrid NF/FF system has recently been installed in the existing dual reflector CPTR. The installed system has been designed to perform spherical, cylindrical and planar NF measurements in the broad frequencies range 0.4-50 GHz.

I. INTRODUCTION

The ESTEC Compact Payload Test Range (CPTR) has recently been updated with a Near Field (NF) system, provided by MVG, with the purposes of extending its operation bandwidth and improving the measurement accuracy [1]-[4]. Since the recent update the facility has been renamed Hybrid ESA RF and antenna Test Zone (HERTZ). As shown in Figure 1. , the ESTEC facility is now a “Hybrid” system hosting the already existing dual reflector compact system and a NF system able to perform spherical, cylindrical and planar NF measurements. The dual reflector system generates a 5m x 7m x 5m (L x W x H) Quiet Zone in the 3.4-20.0 GHz frequency range. The NF system is instead capable to cover a broader frequency range going from 400 MHz to 50 GHz with a maximum planar acquisition area of approximately 9m x 9m (W x H). With the mentioned upgrade the agency is now capable of measuring satellite systems covering services down in frequency to 400MHz and up to 50 GHz.

As part of the system upgrade, MVG has also provided the agency advanced post-processing tools with echo reduction [5]-[6] and diagnostic capabilities [6]. The diagnostic capabilities of the MVG INSIGHT [6] software are exploited in this paper to perform the study of the coupling between different antennas installed on a satellite.



Figure 1. Hybrid ESA Rf and antenna Test Zone (HERTZ) at ESA-ESTEC.

The commercially available INSIGHT software [6] implements the so called equivalent current approach (EQC) / Inverse Source Technique [7]-[10] that provides advanced antenna measurement post-processing. Based on the acquired Near Field (NF) or Far Field (FF) data, the equivalent electric and magnetic radiating currents are determined on an arbitrary shaped reconstruction surface conformal to the test object. The availability of the equivalent currents is a key point for the analysis/post-processing of measured antennas since they can be used to obtain unique diagnostic information and also for other purposes such as spatial filtering [9]-[10], NF/FF transformation and source for numerical computation [11].

The INSIGHT processing tool has been used to assess coupling between antennas and satellite structure on the GALILEO FOC satellite produced by OHB.

In particular the NF measurements of an UHF antenna installed on the top part of the satellite has been taken into account for the analysis. The choice of such antenna among the others lies on the fact that its measured radiation pattern on the satellite was slightly different with respect to the one measured in a stand-alone configuration. A non negligible coupling with other antennas were thus expected. A similar measurement of an L-band antenna located in the same area of the satellite where the UHF antenna is placed has been analyzed as well.

II. SATELLITE AND NF MEASUREMENT DESCRIPTION

The GALILEO FOC satellite consists of several antennas working at different frequencies. Each antenna mounted on the satellite has been measured using a Planar NF (PNF) or Spherical NF (SNF) geometry depending on the antenna characteristics. A photo of the spacecraft during measurement in the ESTEC range is shown in Figure 2.

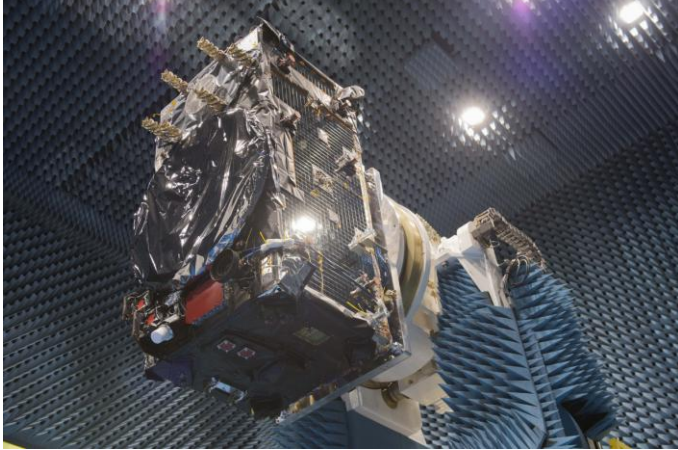


Figure 2. GALILEO FOC Satellite undergoing antenna farm testing at ESTEC.

With reference to Figure 2. , the satellite antenna farm is composed by:

- UHF Search and Rescue Antenna (Sarant UHF), the array of helixes located in the top part of the satellite;
- L-Band Search and Rescue Antenna (Sarant L-Band) located within the Sarant UHF;
- Navigation antenna (Navant), the big circular antenna located in the central part of the satellite;
- Mission antenna (Misant), the horn antenna located in the bottom-right part of the satellite;
- Omni-directional antenna located in the bottom-left part of the satellite.

The PNF measurements of the two Search and Rescue antennas have been taken into account for the coupling analysis with the other antennas. The size of the planar scanner used for the measurement of the Sarant UHF is $(X \times Y) = (5.78 \times 5.78)$ m and the distance from the satellite is 2.25m. Instead, concerning the Sarant L-Band, the size of the planar scanner is $(X \times Y) = (5.9 \times 5.9)$ m and the distance from the satellite is 1.38m. For both measurements a standard half-wavelength sampling has been considered along both scanning axes. Furthermore, the center of the scanning plane has been aligned with the center of the fed antennas.

The outcomes of the coupling analysis performed using the Equivalent Currents computed by INSIGHT from the PNF measurement are shown in the next section.

III. COUPLING ANALYSIS WITH EQUIVALENT CURRENTS

The coupling analysis performed with INSIGHT is reported in this section. In particular, results obtained when the Sarant UHF is fed are shown in the first paragraph (A) while the results obtained when the Sarant L-Band is fed are shown in the second paragraph (B).

A. Sarant UHF

In order to understand the coupling phenomena between the different satellite antenna, the Equivalent Currents have been computed on a equivalent geometry conformal to the spacecraft. The electric currents computed from the PNF measurement of the full satellite with the fed Sarant UHF are shown in Figure 3.

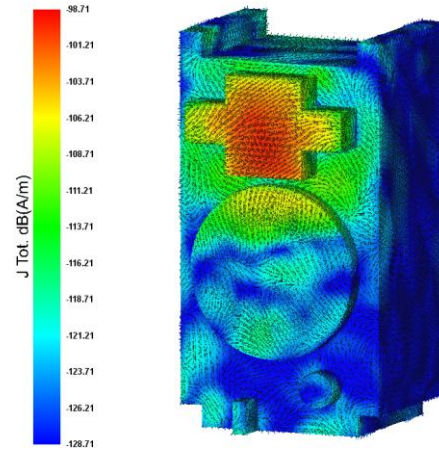


Figure 3. Equivalent electric current on the satellite when the Sarant UHF is fed.

As can be seen the chosen equivalent geometry is mainly composed by a large box enclosing the body of the satellite. Furthermore, on the top part of such box, four additional equivalent surfaces enclosing the different antennas mentioned in the previous section have been created. In particular such equivalent surfaces are:

- a cross-shaped surface on the top part enclosing the two Search and Rescue antennas;
- a big cylindrical surface on the central part enclosing the Navant;
- a small cylindrical surface on the bottom-right part enclosing the Misant;
- a small box on the bottom-left part enclosing the omni-directional antenna.

The equivalent electric currents are, as expected, mainly concentrated on the equivalent surface associated to the Sarant antennas. Nevertheless, it is easy to observe that a non-negligible portion of currents flows on the upper part of the Navigation antenna. Minor contributes of induced equivalent

currents are instead identified on the Misant and omni-directional antennas.

In order to understand the polarization characteristic of the currents induced on the Navant, the equivalent electric currents have been decomposed in right-hand (RHCP) and left-hand (LHCP) circular polarized components. Such a decomposition is shown in Figure 4. As can be seen, the induces currents are mainly RHCP as the currents associated the fed antennas. The strongest impact of such induced currents is thus expected on the co-polar radiation pattern.

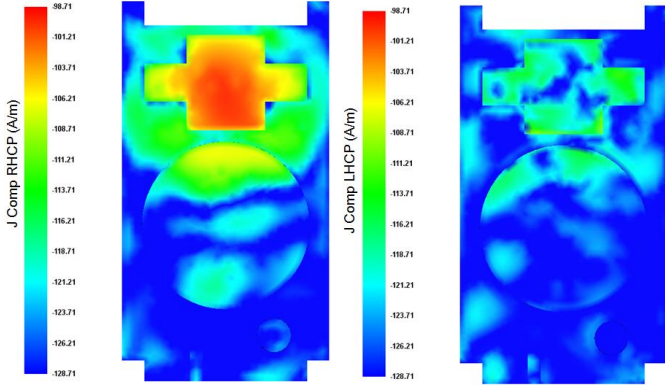


Figure 4. RHCP and LHCP equivalent electric current on the satellite when the Sarent UHF is fed.

With the purpose of understanding the influence of the discovered induced currents on the radiation pattern a spatial filtering [9]-[10] has been applied on the satellite equivalent currents. In particular, as illustrated in Figure 5, the induced equivalent currents on the Navant have been first switched-off (see Figure 5. left) and then only the induced currents on the Navant have been turned-on (see Figure 5. right).

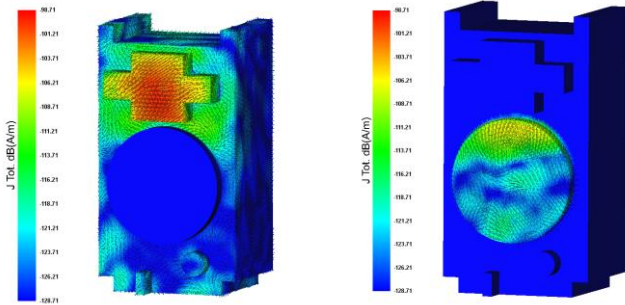


Figure 5. Spatial filtering of the Navigation Antenna.

The radiation patterns along the horizontal cut computed from the two current distributions shown in Figure 5. are shown in Figure 6. together with the pattern radiated from the currents distribution without any spatial filtering applied. In such plot solid lines are the RHCP components while dashed lines are the LHCP components.

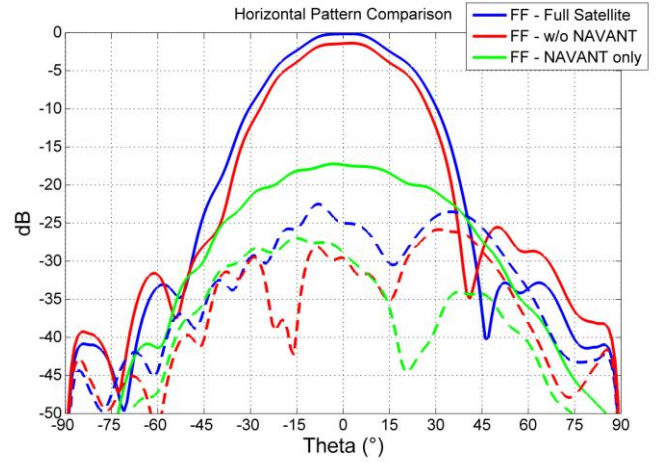


Figure 6. Sarant UHF pattern comparison: FF from full EQC (blue traces); FF with Navant switched-off (red traces); FF with only Navant turned-on (green traces).

As expected, the RHCP pattern radiated only by the equivalent currents induced on the Navant (solid green trace) is relatively high (up to approximately -17.5dB in the main beam area). As a consequence, the radiation pattern of the Sarant UHF is sensibly modified as observable comparing the solid-blue and solid-red traces.

B. Sarant L-band

An analysis similar to the one relative to the Sarant UHF has been performed also on the Sarant L-Band.

The equivalent electric currents computed starting from the PNF measurement of the full satellite with the fed Sarant L-Band are shown in Figure 7. As can be seen, the same equivalent geometry conformal to the satellite used in the previous analysis has been considered.

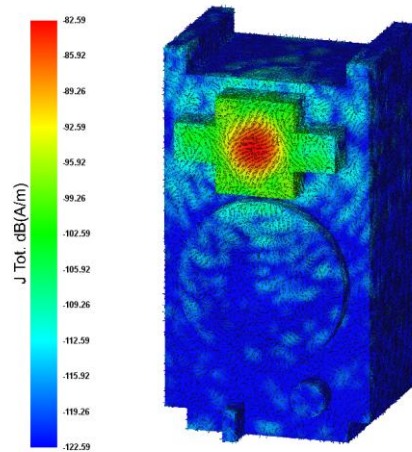


Figure 7. Equivalent electric current on the satellite when the Sarant L-band antenna is fed.

The equivalent currents are now mainly concentrated on the central part of the cross-shaped surface where the fed antenna is located. It is also observed that in this case the currents induced on the Navigation antenna, and also in the remaining part of the satellite, are less strong with respect to the previous situation where the Sarant UHF were fed.

The decomposition of the equivalent currents in terms of RHCP and LHCP components shown in Figure 8. confirms that the coupling phenomena when the Sarant L-Band is fed are definitely less important with respect to the previous scenario.

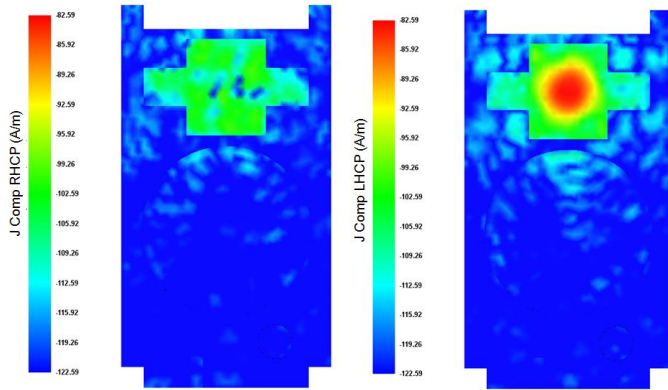


Figure 8. RHCP and LHCP equivalent electric current on the satellite when the Sarant L-band antenna is fed.

Starting from the computed equivalent current two spatial filtering have been applied even in this case switching-off the Navant and turning-on only the Navant. The radiation patterns along the horizontal cut computed from the two sets of spatial filtered current distribution are shown in Figure 9. together with the pattern radiated from the currents distribution without any spatial filtering applied. In such plot solid lines are the LHCP components while dashed lines are the RHCP components.

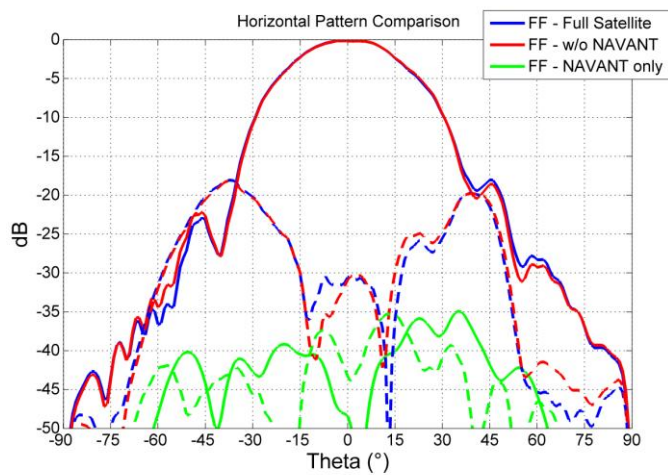


Figure 9. Sarant L-Band pattern comparison: FF from full EQC (blue traces); FF with Navant switched-off (red traces); FF with only Navant turned-on (green traces).

The pattern radiated only by the Navant is in this case relatively low (maximum value is around -35dB). Consequently, the pattern radiated by the full set of currents (blue traces) and the pattern obtained switching-off the Navant (red traces) are in good agreement, confirming that the interaction between the Sarant L-Band with the Navant is very low.

IV. CONCLUSION

The analysis of coupling phenomena between antennas installed on the GALILEO FOC satellite produced by OHB and measured in the new HERTZ system at ESA/ESTEC has been presented in this paper. The analysis has been performed using the EQC technique implemented in the commercially available software INSIGHT. The analysis performed on the UHF Search and Rescue antennas allowed to identify non-negligible currents flowing on the underlying Navigation antenna resulting in a modification of the radiation pattern. Minor coupling effect has instead been identified from the analysis of the L-Band Search and Rescue antenna. Information derived from this analysis could be exploited in the design of next generation of GALILEO satellite in order to optimize the position of antennas on farm.

REFERENCES

- [1] S. Burgos, M. Boumans, P. O. Iversen, C. Veighlhuber, U. Wagner, P. Miller, "Hybrid test range in the ESTEC compact payload test range", 35th ESA Antenna Workshop on Antenna and Free Space RF Measurements ESA/ESTEC, The Netherlands, September 2013
- [2] S. Burgos, P. O. Iversen, T. Andersson, U. Wagner, T. Kozan, A. Jernberg, B. Priemer, M. Boumans, G. Pinchuk, R. Braun, L. Shmidov, "Near-Field Hybrid Test Range from 400 MHz to 50 GHz in the ESTEC Compact Payload Test Range with RF upgrade for high frequencies", EUCAP 2014
- [3] A. Geise, H.-J. Steiner, J. Hartmann, M. Paquay, L. Salghetti Drioli, "Performance Analysis of Near Field Test System in Existing Compact Range Environment",
- [4] A. Geise, H. J. Steiner, J. Hartmann, L. Salghetti Drioli, M. Paquay "Analysis of the Applicability of Near Field Scanners into Existing Compact Test Ranges"
- [5] http://www.mvg-world.com/products/field_product_family/antenna-measurement-2/mv-echo
- [6] http://www.mvg-world.com/products/field_product_family/antenna-measurement-2/insight
- [7] J. L. Araque Quijano, G. Vecchi. Improved accuracy source reconstruction on arbitrary 3-D surfaces. *Antennas and Wireless Propagation Letters, IEEE*, 8:1046–1049, 2009.
- [8] L. Scialacqua, F. Saccardi, L. J. Foged, J. L. Araque Quijano, G. Vecchi, M. Sabbadini, "Practical Application of the Equivalent Source Method as an Antenna Diagnostics Tool", AMTA Symposium, October 2011, Englewood, Colorado, USA
- [9] J. L. A. Quijano, G. Vecchi, L. Li, M. Sabbadini, L. Scialacqua, B. Bencivenga, F. Mioc, L. J. Foged "3D spatial filtering applications in spherical near field antenna measurements", AMTA 2010 Symposium, October, Atlanta, Georgia, USA.
- [10] L. J. Foged, L. Scialacqua, F. Mioc, F. Saccardi, P. O. Iversen, L. Shmidov, R. Braun, J. L. Araque Quijano, G. Vecchi "Echo Suppression by Spatial Filtering Techniques in Advanced Planar and Spherical NF Antenna Measurements ", AMTA, Oct 2012, Seattle, Washington, USA
- [11] L. J. Foged, L. Scialacqua, F. Saccardi, F. Mioc, D. Tallini, E. Leroux, U. Becker, J. L. Araque Quijano, G. Vecchi, "Bringing Numerical Simulation and Antenna Measurements Together", ", IEEE Antennas and Propagation Society International Symposium, July 6-11, 2014.